



University  
of Science and Technology  
in Zewail City

# Diagnosis of ASD using fMRI: A Computer-Aided Approach

By: Alaa Mohamed Mostafa Elmansy

In partial fulfilment of requirements for the degree of  
Bachelor of Science in  
Biomedical Sciences  
University of Science and Technology at Zewail City

Supervisor  
Prof. Dr. Doaa Shawky

Date of submission  
3<sup>th</sup> of June 2025



مدينة زويل للعلوم والتكنولوجيا  
Zewail City of Science and Technology

## Abstract

This project aims to address the challenges of diagnosing the Autism Spectrum Disorder (ASD) accurately, which is a neurodevelopmental disorder that affects social activity, communication, and repetitive behaviour. The current diagnosis depends on the subjective behavioural assessment, and there is no established medical test. Misdiagnosis can raise significant issues and make the patient more susceptible to depression, self-harm, and eating disorders. Recent studies suggest that ASD is associated with changes in brain organization and neural connectivity, revealing a potential diagnosis using brain image data such as functional magnetic resonance imaging (fMRI). This project suggests that using Machine learning (ML) and Deep learning (DL) to analyze this functional brain network imaging data can be a promising method to distinguish between typical developing (TD) controls and ASD persons. This study proposes an automated diagnostic method utilizing the time series data for regions of interest identified by Bootstrap Analysis of Stable Cluster (BASC) atlas for 340 subjects, including 170 subjects diagnosed. The methodology implies constructing a connectivity pairwise matrix using Spearman correlation and Transfer entropy matrices. The Spearman correlation matrix for each subject will be used with ML models. For the DL, Transfer entropy (TE) matrices will be used as a connectivity matrix, then the sliding window technique to analyze functional brain dynamics and long short-term memory will be used for classification. The results show .72 and .75 accuracy for the support vector machine and logistic regression, respectively. SHAP value analysis indicating key brain regions contributing to classification, such as Left-Fusiform-Left-PrimMotor. The LSTM model and sliding window technique require higher computational complexity to proceed. This project investigated the potential use of ML and DL for ASD diagnosis, and indicated the brain regions contributing to this disorder, while highlighting the need for further refinement of DL approaches to capture dynamic brain interactions effectively.

## Acknowledgment

First, I want to send my sincere thanks to Allah for guiding me all the time, making me able to continue each day, and for his uncountable blessings. I owe him lifelong gratitude. Second, I am grateful to Dr. Doaa Shawky, whose support, guidance, and kindness had an incredible influence on my journey. Her way of dealing has been a lighthouse blessing, making me relaxed and able to investigate, learn, and gain new skills.

Second, I owe a great deal to my Zewail City instructors, especially those in the Department of Biomedical Sciences. My academic path has been much influenced by your unfailing support and priceless insights. I am especially appreciative of Dr. Eman Badr, whose encouragement and guidance have established and sharpened my academic research skills and insights. Thanks to everyone of you for the great drift in influence you made on my path.

Remembering all that I went through, I am grateful to everyone in my family for their unconditional support and love. Your support and encouragement have been a constant source of consolation in whatever I face in my life. I appreciate you being my inspiration and rock-solid source of support on this incredible trip. No words can express how much I am grateful for being a part of this incredible family. All I can say is that if I have the right to choose, I will never find a better one.

Special thanks also to the incredible TAs and RAs who made this journey easier and better: Ms. Shrook Badwy, Ms. Ereeny Adel, and Ms. Jihad Masood. Your friendship and unfailing support have been priceless, and I am very grateful for your guidance.

A four-year journey of struggle and experience wouldn't have been this amazing and fruitful without my dearest roommate, Nada Nabil. Your heart of gold, joy, and the moments we shared will forever guide my way. We have come a long way from where we began our adventure and friendship. I also want to thank Raghda Salah, Mariam Hussien, Dina Allam, Mayar Hatem, Naglaa Mohamed, Engy Wael, and Aisha Badr. Each of you contributed to making this experience not only academically rewarding but also filled with pleasant memories. The sense of hospitality, sisterhood, and compassion I found in all of you has touched my heart, opened my eyes, and allowed me to see life from your bright

perspectives. You were my backbone and shelter, supporting me as I faced life's obstacles. Thank you for illuminating my hope and aspirations.

I want to thank all my colleagues for their support. Especially, Alaa Elshazly, Hayam Walled, Mariam Waleed, Nada Sameh, Basmala Medhat, Hanin Hamdy, Amany Ibrahim, and Amira Tantawy. You have elevated my skills; your generosity and help have made this road less intimidating and more rewarding. I am incredibly appreciative of every one of you for your unfathomable contributions to my accomplishments.

Gantt Chart

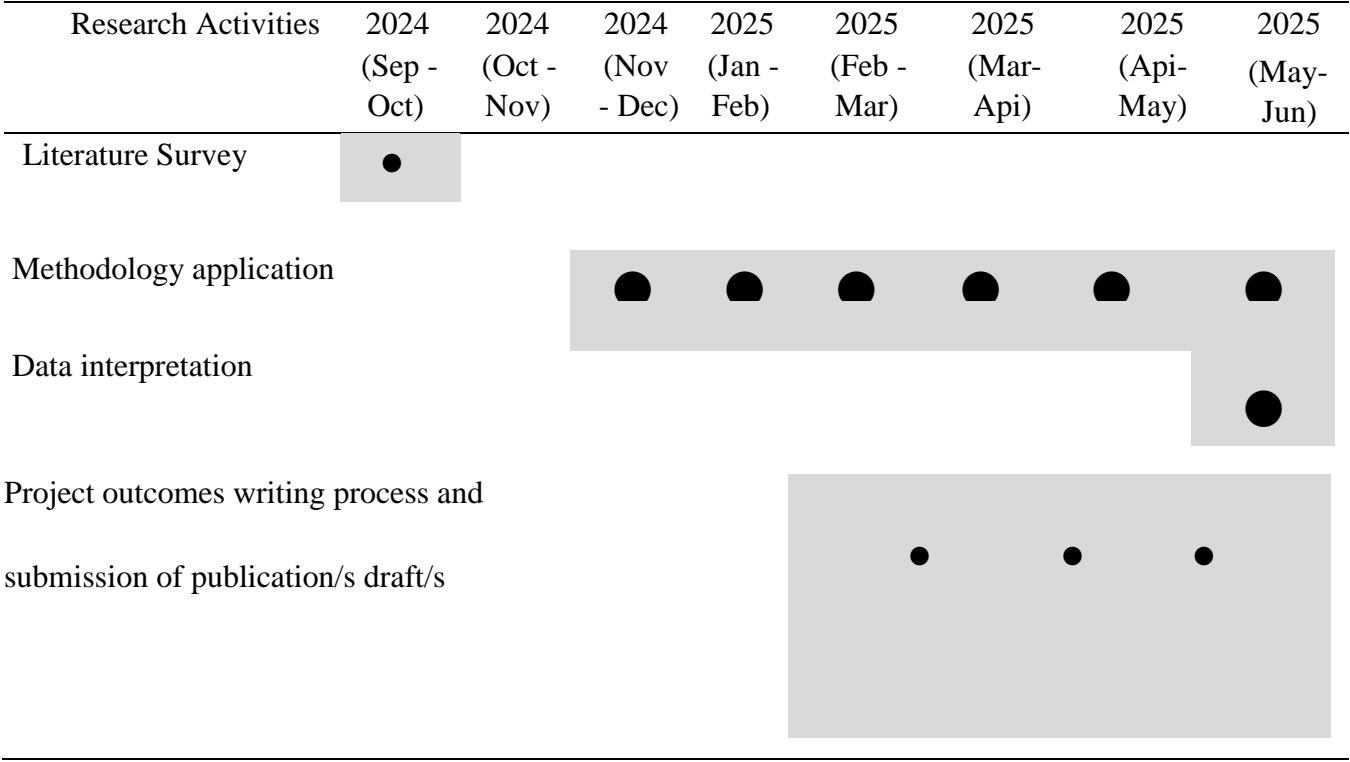


## *Table of Contents*

<b>List of abbreviations.....</b>	<b>Error! Bookmark not defined.</b>
Autism Spectrum Disorder .....	7
<b>1. Chapter One: Introduction.....</b>	<b>9</b>
1.1. Background .....	9
1.2. Research Background.....	9
1.2.1. Problem Statement .....	10
1.2.2. Research Question .....	10
1.2.3. Research Aim .....	10
1.2.4. Research Outcome:.....	11
<b>2. Chapter Two: Literature Review.....</b>	<b>12</b>
2.1. Autism Spectrum Disorder (ASD) and Its Diagnosis: .....	12
2.2. fMRI for Investigating Brain Function in ASD .....	12
2.3. Brain Parcellation and Atlas-Based Analysis:.....	12
2.3.1. Standard Anatomical and Functional Atlases .....	13
2.3.2. Data-driven Atlases: BASC.....	13
2.4. Functional Connectivity (FC) and ML Classification:.....	13
<b>3. Chapter Three: Materials and Methods .....</b>	<b>16</b>
3.1. Data collection.....	16
3.2. Machine learning approach: .....	16
3.2.1. Preprocessing and Feature Extraction .....	16
3.2.2. Dimensionality Reduction:.....	17
3.2.3. Machine Learning Models: .....	17
3.2.3.1. Model Evaluation .....	18
3.2.4. Interpretability Analysis with SHAP:.....	18
3.3. Deep learning approach:.....	18
3.3.1 Data Preparation and Preprocessing.....	18
3.3.2 LSTM Network Architecture and Training.....	19
3.3.3 Model Evaluation .....	20
3.3.4 Interpretability (Not Applied) .....	20
Table 2: Hyperparamters for LSTM used for GridSearch. ....	20
<b>4. Chapter Four: Results and Discussion .....</b>	<b>21</b>
<b>5. Chapter Five: Conclusion and Recommendations:.....</b>	<b>26</b>
<b>References .....</b>	<b>27</b>

### ***List of Tables***

Table 1: Hyperparameters used for SVM and LR models. ....	17
Table 2:Hyperparamters for LSTM used for GridSearch.....	20

### ***List of Figures***

Figure 1: The ROC curve comparing SVM and LR Classifiers for ASD .....	22
Figure 2: SHAP Vale plot indicating the top contributing features on ASD and TD classification. ....	24
Figure 3: The Bar chart represents the mean impact of features on the model output based on the SHAP value. ....	25

### *List of abbreviations*

Abbreviations	Meaning
ASD	○ Autism Spectrum Disorder
ML	Machine learning
fMRI	Functional Magnetic Resonance Imaging
DL	Deep Learning
TE	Transfer Entropy
DTI	Diffusion Tensor Imaging
EEG	Electroencephalogram
rs-fMRI	Resting-state fMRI
FC	Functional Connectivity
ROIs	Regions of Interest
AAL	Automated Anatomical Labeling
BASC	Bootstrap analysis of stable clusters
SVM	Support Vector Machine
LR	Logistic Regression
RNN	Recurrent Neural Networks
LSTM	Long Short-Term Memory

Abbreviations	Meaning
---------------	---------



ABIDE	Autism Brain Imaging Data Exchange
PCP	Preprocessed Connectomes Project
PCA	Principal Component Analysis
KSG	Kraskov, Stögbauer, and Grassberger
FPR	False Positive Rate
TPR	True Positive Rate

## ***1. Chapter One: Introduction***

### **1.1. Background**

Autism spectrum disorder (ASD) is one of the complicated, multifactorial neurodevelopmental disorders that can happen due to the genetic makeup and appear in childhood, usually in the first 3 years of life. It affects the person in many aspects, including difficulty in social communication, repetitive patterns, and can affect the learning journey [1- 3]. The multifactorial nature of autism, with its different symptoms, makes its diagnosis challenging. Lacking of specific medical test, unlike other medical conditions, the diagnosis relies on personal observation for the patient's behaviour, social interaction, activities, interests, and communication by an expert [4].

The possibility of misdiagnosis is high and can have a negative impact on the child, the family, and the educational system. Also, the late diagnosis can lead to the same negative impact, including increasing the risk of depression, self-harm, and eating disorders. Misdiagnosis can also happen due to the overlapping symptoms or even co-occurrence between ASD and other disorders. This makes it important to find a reliable quantitative method for ASD diagnosis, such as functional brain imaging [1], [4].

### **1.2. Research Background**

Previous studies suggest that autism can be characterized by variation in brain organization. Neural connectivity arose as a common method to develop a technique to diagnose and investigate the different symptoms associated with this disorder. Functional magnetic resonance imaging is widely used nowadays to achieve this goal. Previous research utilizing fMRI suggested that input to brain regions is cut off, revealing an activation and functional correlation decrease for the sensory brain areas [5]. Furthermore, it shows an abnormal activation in the parietal cortex, which is the brain part responsible for visuospatial and sensory processing [6], [7]. Moreover, during the rest-state, the medial prefrontal cortex regions, which are responsible for decision making and attention, are suppressed in the ASD individual. They also investigated other regions, including the rostral anterior cingulate cortex and the posterior cingulate cortex, which plays a crucial role in emotional, cognitive, and learning processes. The midline of the resting network of an ASD person shows less activity than that of a typically developing besides deactivation for other insignificant tasks [8]. In addition to the

functional differences, an ASD person also shows structural differences, such as early overgrowth of white matter with reduction in adolescence. The analysis of diffusion tensor imaging (DTI) highlighted a disorganization of white matter paths. These investigations collectively suggest that the functional and structural variations between normal and ASD can provide a precise diagnosis [9],[10].

Electroencephalogram (EEG) and fMRI can provide information on brain anatomical organization. EEG has a precise temporal resolution, while fMRI can provide high spatial resolution to analyse spatial brain dynamics [11],[12],[13]. fMRI captures Blood Oxygenation Level-Dependent (BOLD) signals through time as three-dimensional images. When the deoxyhemoglobin rate decreases, the NMR signal increases, which represents the hemodynamic response function, which is determined by the pixel intensity of the fMRI image. Each anatomical brain region is represented by a voxel, which is a cube of an fMRI image with a BOLD time series. This BOLD is then being used to classify the ASD individual [14, 15]

### *1.2.1. Problem Statement*

Given the diagnosis challenges mentioned above, the variant symptoms, lack of medical test, the current diagnosis depends on expert observation that can lead to misclassification and late diagnosis [4]. While machine learning and deep learning methods are being used in this topic, many of them use only one connectivity metric, such as Pearson correlation, and may miss the complex organization of the brain network. In addition to a lack of interpretability, and use of a small dataset [16,17,18].

### *1.2.2. Research Question*

Can machine and deep learning models differentiate effectively between a normal and an ASD person and identify the reasons associated with this disorder?

### *1.2.3. Research Aim*

This research aims to diagnose ASD using a computer-aided approach with machine and deep learning, utilizing fMRI data. Also, make medical interpretability for the causes and affected brain parts.

#### *1.2.4. Research Outcome:*

This study successfully proposed a computer-aided approach for ASD diagnosis using fMRI data, revealing several insights regarding machine and deep learning in this field.

Machine learning output: the use of Spearman correlation matrix with SVM and LR gives .72 and .75 accuracy. In addition to high values for the Area Under the Curve (AUC), with .8 for SVM and .82 for logistic regression. The SHAP value indicated main brain regions contributed to the classification, including Left-Fusiform-Left-PrimMotor, Left-Hippocampus-Left-PrimMotor, Left-Sec Visual-Outside defined BAS1, Left-PrimMotor-Outside defined BAS1, Left-FrontEyeFields-Outside defined BAS1, which can be used for further investigation as biomarkers.

However, the deep learning models with the sliding window technique for data augmentation are still challenging and need high computational power to perform the analysis.

## ***2. Chapter Two: Literature Review***

### **2.1. Autism Spectrum Disorder (ASD) and Its Diagnosis:**

ASD is a complicated neurodevelopmental disorder that has several symptoms, including a lack of social communication skills, in addition to restricted behaviour, desires, and activities [19]. The early diagnosis of ASD is important for making a suitable intervention, however, the current diagnosis still relies on behavioural observation, which is not accurate and time-consuming [20]. There is a high need to discover the biomarkers and find an objective diagnostic method. fMRI, a brain imaging technique that measures brain activity by capturing the changes in blood flow, has become a promising technique for ASD diagnosis [21]. Machine and deep learning provide a flexible model that can capture the complex patterns in this high-dimensional fMRI data. The previous studies have made two ML approaches for ASD diagnosis; the first is based on static functional connectivity with traditional classifiers, and the second is more advanced DL models that rely on dynamic effective connectivity [22].

### **2.2. fMRI for Investigating Brain Function in ASD**

Resting-state fMRI (rs-fMRI) is performed without requiring the patient to perform a specific task; however, it can measure the brain activity and functional organization, which makes it a valuable method for ASD diagnosis [23]. This makes it applicable for different people, especially for ASD people who already have difficulties in performing certain tasks. One of the main findings is the alternation of functional connectivity (FC), which means the different behavior of temporal correlation of BOLD signals between the different brain regions, which can be under- or over-connectivity according to the brain network involved [24].

### **2.3. Brain Parcellation and Atlas-Based Analysis:**

To perform a fruitful fMRI analysis, the brain is divided into parcels known as regions of interest (ROIs). This process involves using atlases that provide predefined ROIs based on the brain anatomy, data-driven clustering, or functional boundaries.

- *2.3.1. Standard Anatomical and Functional Atlases*

There are well-known atlases that provide anatomically and functionally derived ROIs, such as the Automated Anatomical Labeling (AAL) atlas [25]. They enable the extraction of mean time series from brain regions for use in connectivity analysis [26].

- *2.3.2. Data-driven Atlases: BASC*

- Bootstrap analysis of stable clusters (BASC) is a data-driven approach for parcellation. It is a k-means clustering-based algorithm that randomly samples the data several times using bootstrapping, then clusters each of these resampled datasets and investigates the frequently grouped data points across the samples [27]. This reveals if the clusters are reliable or contain artifacts. This makes it a reliable method for extracting the ROIs for subsequent connectivity matrices [27], [28].

- **2.4. Functional Connectivity (FC) and ML Classification:**

After constructing the ROIs using the BASC atlas, FC is being calculated between all pairs of ROIs.

- 2.4.1. Spearman Correlation for FC Estimation:*

Unlike Pearson correlation, which is commonly used for FC computing, Spearman correlation is a non-parametric alternative that is better for non-Gaussian distributions and capturing the monotonic relationships between time series [29]. The resulting matrices represent the correlation coefficient between each pair of ROIs, which resemble the input features for the machine learning models.

- 2.4.2. Traditional ML Classifiers: SVM and Logistic Regression:*

One of the widely used machine learning models for neuroimaging research is the support vector machine (SVM) and logistic regression (LR). SVM main goal is to separate the classes by finding the best hyperplane in the high-dimensional feature space. It shows a promising interpretability and applicability in neurodevelopmental research. Furthermore, LR is showing a respected result in binary outcome prediction probability in addition to being a linear model. It's frequently used in ASD classification research. However, this ML approach has a lot of challenges,

including the curse of dimensionality, and can miss the dynamic changes due to the static nature of FC because it takes the average connectivity through the scan duration [4 from ch1], [30].

## 2.5. Dynamic and Effective Connectivity with Deep learning

The previous traditional machine learning approach with static FC measures misses the directed flow of information and the dynamic brain nature which can give a better understanding of the disease and better classification.

### 2.5.1. Transfer Entropy for Effective Connectivity:

It is a leading method widely used for connectivity measures, which is the information-theoretic measure. TE can indicate the non-linear interaction and quantify the directed transfer of information between two time series. It's being calculated as mentioned in the next equation, Eq.1[31],[32], [33].

$$TE_{Y \rightarrow X}(\tau) = \sum_{i=1}^N P(x_{t+\tau}^i, x_t^i, y_t^i) \log \frac{P(x_{t+\tau}^i | x_t^i, y_t^i)}{P(x_{t+\tau}^i | x_t^i)} \quad (1)$$

where:

- $TE_{Y \rightarrow X}(\tau)$  denotes the transfer entropy from  $Y$  to  $X$  at time lag  $\tau$ .
- $x_t^i$  and  $y_t^i$  represent samples from time series  $X$  and  $Y$  respectively.
- $N$  is the total number of samples.
- $P(x_{t+\tau}^i, x_t^i, y_t^i)$  is the joint probability distribution of  $x_{t+\tau}^i$ ,  $x_t^i$ , and  $y_t^i$ .
- $P(x_{t+\tau}^i | x_t^i, y_t^i)$  is the conditional probability distribution of  $x_{t+\tau}^i$  given  $x_t^i$  and  $y_t^i$ .
- $P(x_{t+\tau}^i | x_t^i)$  is the conditional probability distribution of  $x_{t+\tau}^i$  given  $x_t^i$ .

It overperforms Spearman correlation since it's not only non-linear but also can capture the directional influences between brain regions[32], [33].

### 2.5.2. Sliding Window Approach for Dynamic Analysis

Since small datasets are a common issue in neurodevelopmental diseases, the sliding window can be a useful method for data augmentation. It can indicate the time-varying nature of brain connectivity. In this technique, the fMRI is divided into shorter windows, overlapping or nonoverlapping, and then the connectivity matrix is calculated for each window. The output is a series of connectivity matrices that represent the brain dynamics. previous research implied it with recurrent neural networks and other deep learning models [4 ch1], [31].

### *2.5.3. Long Short-Term Memory (LSTM) for Sequential Data:*

Recurrent Neural Networks (RNN) are well-suited for fMRI classification and analysis of series of connectivity matrices obtained from the sliding window, especially Long Short-term Memory (LSTM) networks. It has a high performance in investigating the temporal dynamics of brain activity. The previous research utilizing LSTM in this context shows higher performance than traditional models and can identify biomarkers since the model learned how patterns of directed information flow over time [31], [34], [35].



### 3. Chapter Three: Materials and Methods

#### 3.1. Data collection

The time series matrices of rs-fMRI data represented the 122 brain regions extracted using BASC atlas for 242 ASD and 258 TD were obtained from [Diagnosis of autism spectrum disorder based on functional brain networks and machine learning | Scientific Reports](#). This data is preprocessed with a .5 Hz band-pass filter. The original data is the preprocessed version of the Autism Brain Imaging Data Exchange (ABIDE) with 300s BOLD time series and provided by the Preprocessed Connectomes Project (PCP) dataset 47. The PCP preprocessing pipeline includes cut time correction, motion correction, intensity normalization, and removal of artifacts such as breathing, heartbeat, and head motion.

A random sample of 170 subjects for both ASD and TD was used in this study, with a fixed seed (`np.random.seed(42)`) for reproducibility

#### 3.2. Machine learning approach :

##### ○ 3.2.1. Preprocessing and Feature Extraction

The time-series matrices were used to extract the connectivity matrices. A Spearman connectivity matrix was calculated for each subject. The Spearman rank correlation was chosen due to its robustness to non-normally distributed data of fMRI. The calculation was implemented as follows:

- For a given time-series matrix  $T \in \mathbb{R}^{N \times 122}$  (where  $N$  is the number of time points and 122 is the number of ROIs), the Spearman correlation  $\rho$  was calculated for each pair of ROIs  $(i, j)$  where  $i < j$ , resulting in a symmetric  $122 \times 122$  connectivity matrix.
- The upper triangle of the connectivity matrix (excluding the diagonal) was extracted using NumPy's `triu_indices` function, yielding  $122 \times (122 - 1)/2 = 7381$  unique connectivity features per subject.

This was calculated for 340 subjects, resulting in a matrix with dimensions  $340 \times 7381$ , where each row is a subject and the columns represent the connectivity score between pairs of ROI, while ASD

is labeled with 1 and TD is 0. The BASC atlas is used for the nilearn Python package to label the 122 regions.

### ○ 3.2.2. Dimensionality Reduction:

Since the matrix has 7381 features, the Principal Component Analysis (PCA) was used to lower the dimensions and avoid the curse of dimensionality. The pipeline was applied with sklearn as follows

1- Imputation: The NAN values of the feature matrix were imputed using [SimpleImputer(Strategy='mean')]

2- standardization: to obtain zero mean and unit variance using (standardScaler)

3- Principal Component Analysis(PCA): using 50 component (PCA(n\_components=50))

The resulted matrix with dimensions 340\*50 was split into training and testing with ratios of .2: .8 with [train\_test\_split(X\_reduced, labels, test\_size=0.2, random\_state=42)]

### ○ 3.2.3. Machine Learning Models:

Two machine learning models were employed to classify ASD versus TD subjects: SVM and LR. Both models were trained and evaluated using a pipeline that included imputation and standardization to ensure consistency with the preprocessing steps. The two models were trained over parameters obtained from GridSearch over parameters obtained from [31] with values mentioned in Table 1

*Table 1: Hyperparameters used for SVM and LR models.*

SVM	Kernel: Specifies the kernel type to be used in the algorithm	[rbf, linear]
	Gamma: Kernel coefficient	[1e-3, 1e-4]
	C: Regularization parameter	[1, 10, 100, 1000]
LR	C: Each value in Cs describes the inverse of regularization strength	range 0.001 to 1000
	Penalty: Specifies the norm of the penalty	[l1, l2]

#### ■ 3.2.3.1. Model Evaluation

Both models were evaluated using the Accuracy (measure the correctly classified samples), Area under the ROC curve (AUC) (model ability to differentiate between classes), Precision( positive diagnosis that was correct), Recall (ASD correctly classified), Specificity (the TD that correctly classified ).

#### ■ 3.2.4. Interpretability Analysis with SHAP:

To interpret the results and know the regions that contributed to the classification, the SHAP value was used. The SHAP value was calculated for 10 samples with 50 features. The top 20 features name was annotated manually based on the names from [31]. shap. Explanation object was created, then used for visualization and heatmap.

### 3.3. Deep learning approach:

This section details the deep learning methodology employed for ASD vs. TD classification using fMRI-derived transfer entropy (TE) matrices. An LSTM network, implemented using the TensorFlow (version 2.18.0) and Keras (version 3.8.0) libraries, was selected for its ability to model temporal dependencies in sequential data. However, despite the chosen approach, the model did not achieve satisfactory performance, as detailed in the Results section.

#### ○ 3.3.1 Data Preparation and Preprocessing

The input data comprised preprocessed time series (as described in Section 3.1) representing the activity of 122 brain regions ROIs defined by the BASC atlas. These time series served as the basis for computing TE matrices.

- **Transfer Entropy Calculation:** Dynamic brain connectivity was captured by calculating TE matrices using a sliding window approach. Within each window, the `compute_transfer_entropy` function computed TE between all possible pairs of the 122 ROIs. This function uses the `pyinform` (version 0.2.0) library, specifically the `transfer_entropy` function. Before applying this function, the time series data within each window was discretized into 10 discrete states using the `discretize_time_series` function, which employs NumPy's `linspace` and `digitize` functions to create bins and assign time series values to their corresponding bins. This discretization step is crucial because the `transfer_entropy` function in `pyinform` operates on discrete data. The `transfer_entropy` function estimates TE using the Kraskov, Stögbauer, and Grassberger

(KSG) estimator, a widely used method for estimating mutual information and related quantities. A delay of 1 time point (sampling interval of approximately 2 seconds) and a history length (k) of 1 were used. NaN values resulting from TE calculation (which may occur due to limited data or numerical issues) were replaced with 0. The resulting 122 x 122 TE matrices are symmetric because TE is calculated bidirectionally between each ROI pair within the window.

- **Sliding Window Implementation:** The `compute_sliding_te_matrices` function was used to implement the sliding window approach, with:

- **Window size:** 20 time points (~40 seconds of fMRI data)
- **Step size:** 2 time points (~4 seconds)  
These parameters were empirically chosen to balance capturing sufficient temporal context with the need for numerous training samples. Smaller window sizes may miss long-term dependencies; larger sizes reduce sample count and can oversmooth data. A smaller step size yields more windows but increases computation and correlation among windows.

- **Data Handling and Dimensionality Reduction:**

TE matrices were saved as individual .npy files per subject to avoid recomputation. For each window, a feature vector of length 7381 was extracted, representing the upper triangular elements (excluding the diagonal) of each TE matrix.

These vectors formed a 3D array (n\_subjects, n\_windows, 7381). To handle high dimensionality:

- Missing values were imputed using `sklearn.impute.SimpleImputer(strategy='mean')`.
- Data were scaled with `sklearn.preprocessing.StandardScaler`.
- PCA was applied using `sklearn.decomposition.PCA`, retaining the top 50 components. PCA was fitted on the training set and then applied to the training and test sets, reducing features from 7381 to 50 while preserving variance and improving numerical stability.

### ○ 3.3.2 LSTM Network Architecture and Training

The parameters of LSTM were obtained using GridSearch with parameters shown in Table 2.

- **Model Architecture:** Built using `tensorflow.keras.models.Sequential`, comprising:
  - **LSTM Layer:** 128 units (`tensorflow.keras.layers.LSTM`), with `return_sequences=False`, input shape (`sequence_length, 50`).

- **Dropout Layer:** Rate of 0.2 (`tensorflow.keras.layers.Dropout`) for regularization.
- **Dense Layer:** Single unit with sigmoid activation (`tensorflow.keras.layers.Dense`) for binary classification.
- **Model Compilation and Training:**
  - **Optimizer:** Adam (`tensorflow.keras.optimizers.Adam`) with default parameters.
  - **Loss Function:** Binary cross-entropy (`tensorflow.keras.losses.BinaryCrossentropy`).
  - **Metrics:** Monitored using accuracy.
  - The model was trained for 50 epochs with a batch size of 32, employing a validation split of 0.2 to assess performance on unseen data during training and monitor potential overfitting.

### ○ 3.3.3 Model Evaluation

The model's performance was assessed using accuracy, AUC, precision, recall, and specificity on held-out test data.

### ○ 3.3.4 Interpretability (Not Applied)

Since the LSTM model did not yield satisfactory results, interpretability analyses using SHAP values were not conducted. It was deemed unproductive to interpret an underperforming model, as it would not provide meaningful insights into data or misclassification reasons.

*Table 2: Hyperparameters for LSTM used for GridSearch.*

Type of Layer	Tuning hyperparameter	Value
LSTM	—	—
LSTM	dropout	[0.00, 0.05, 0.10, 0.15, 0.20, 0.25, 0.30, 0.35, 0.40, 0.45, 0.50]
LSTM	—	—
LSTM	units	[70, 60, 50, 40]
Dense	- units	3
	- activation	softmax
Adam optimization compile	learning rate	$\min - \text{value} = 1e^{-10}$
		$\max - \text{value} = 1e^{-1}$
		sampling = LOG

■

#### ***4. Chapter Four: Results and Discussion***

The best SVM model parameters:

Best SVM Parameters: {'svm\_\_C': 1000, 'svm\_\_gamma': 0.001, 'svm\_\_kernel': 'rbf'}, which indicates a robust regularized model with a flexible kernel that reduces the bias and variance efficiently.

Best logistic regression model:

Best Logistic Regression Parameters: {'lr\_\_C': 0.001, 'lr\_\_penalty': 'l2', 'lr\_\_solver': 'liblinear'} indicating a highly regularized model, that prevents overfitting with small sample data

The models show an acceptable accuracy of .72 for SVM and .75 for LR, which is accepted in comparison to other literature and can be an effective model for classification. The Area under the curve is shown in Figure 1, the X-axis is the false positive rate (FPR), the Y-axis is the true Positive Rate (TPR), and the dashed line is the random classification performance = .5. The SVM value is .8 and the LR is .82, which indicates a high and better discrimination between the different classes. For the precision, the SVM showed .75 while the LR is .79, which means the LR is slightly outperforming the SVM and means it has fewer false positive results, which is better for the overall performance. The recall for SVM is .68 and LR is .79, which also shows better and higher performance for LR in identifying the actual positive cases, reducing the false negatives. Finally, the specificity is .79 for SVM and .8 for LR, indicating a good ability to identify negatives.

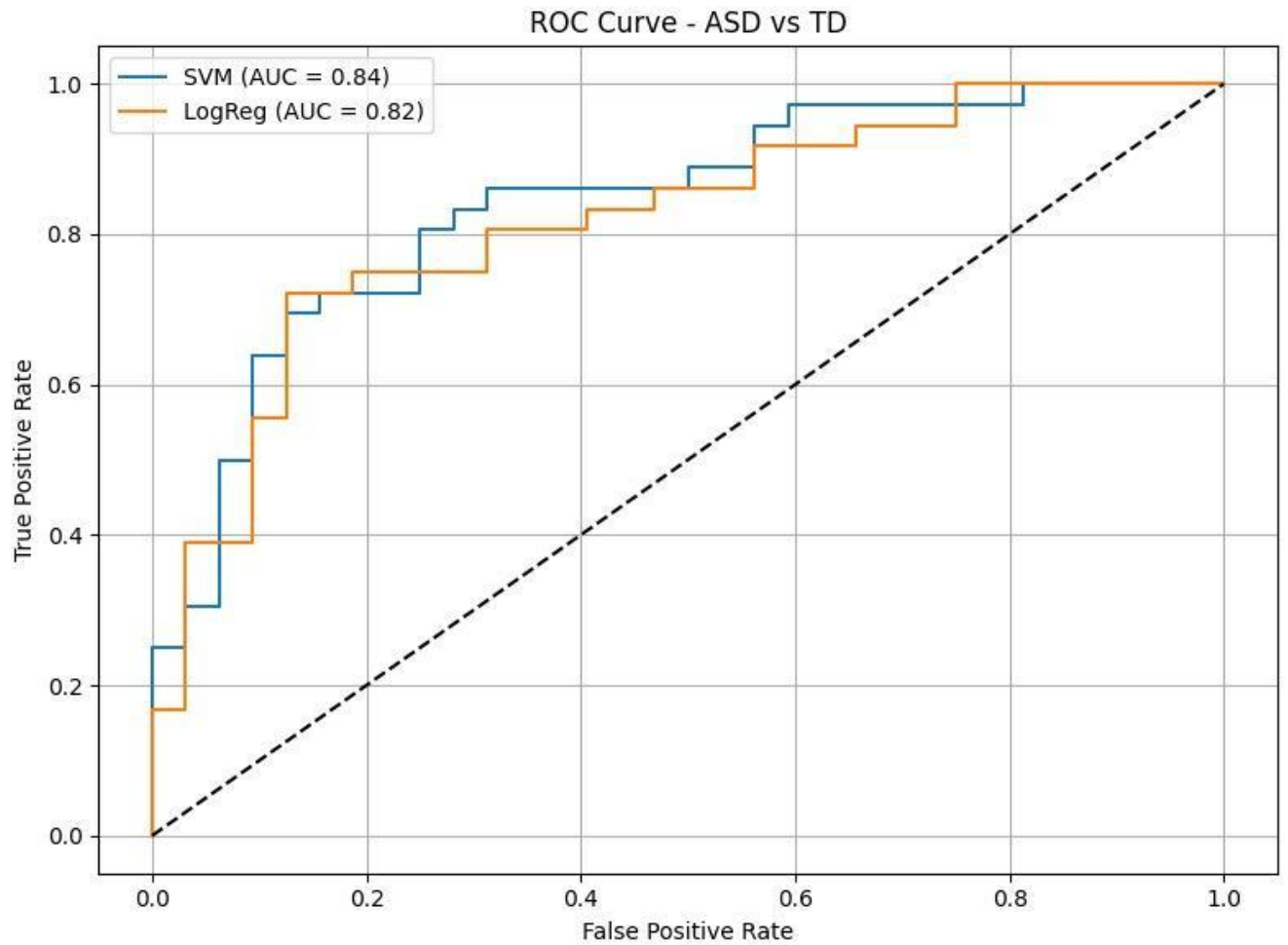


*Figure 1: The ROC curve comparing SVM and LR Classifiers for ASD*

The results of SHAP Value (Figure 2) show the impact of different features on the model output. Each row represents a specific brain region, and blue is low value while pink is high, indicating higher feature impact. Features that drift to the right (positive) increase the probability of being ASD diagnosed, while shifting to the left indicates TD. So the features with higher pink indicate their association with ASD, such as Left-Fusiform-Left-PrimeMotor. The figure shows the names of brain regions such as Left-Fusiform-Left-PrimMotor, Left-Hippocampus-Left-PrimMotor, Left-Sec Visual-Outside defined BAS1, Left-PrimMotor-Outside defined BAS1, Left-FrontEyeFields-Outside defined BAS1, Left-VentPostCing-Outside defined BAS1, Left-Thalamus-Left-PrimMotor, Left-PrimMotor-Outside defined BAS1. The figure also contains ROIs that need further annotation with the appropriate atlas.

The same result was represented by a horizontal bar plot in Figure 3, and it shows that the top features (Left-Fusiform-Left-PrimMotor, ROI31, Left-Hippocampus-Left-PrimMotor, Left-Sec Visual-Outside defined BAS1, ROI24) have the highest mean impact, close to approximately 0.12. Then, the values are decreasing gradually. The Deep learning approach needs higher computational complexity to give the final result.



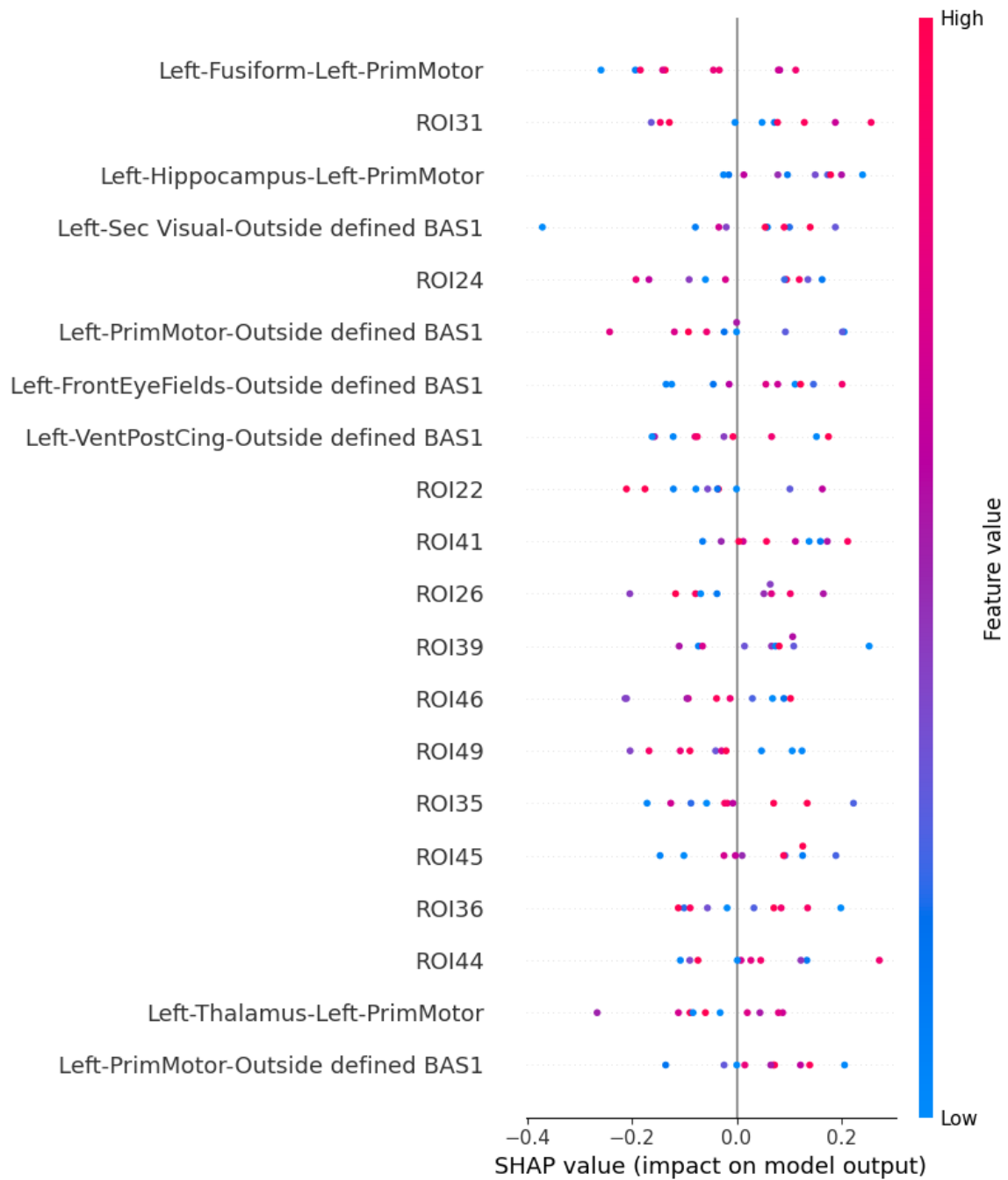
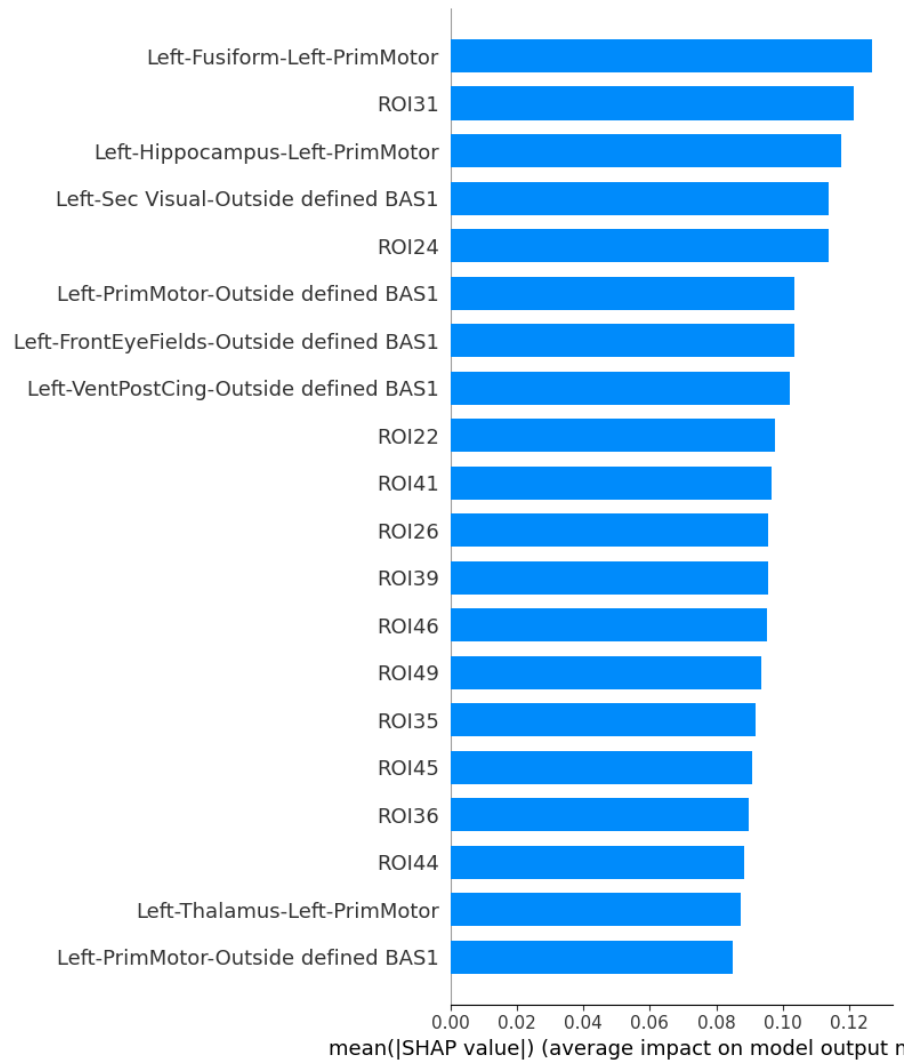


Figure 2: SHAP Value plot indicating the top contributing features on ASD and TD classification.



*Figure 3: The Bar chart represents the mean impact of features on the model output based on the SHAP value.*

## ***5. Chapter Five: Conclusion and Recommendations:***

This project succeeded in developing and evaluating an automated method for ASD diagnosis using fMRI image analysis with machine and deep learning models. The machine learning models show good accuracy, while deep learning still has some limitations due to the computational complexity. The 2 ML models used SVM and LR show an accuracy of 0.75, precision of 0.79, and recall of 0.79 for LR, which is better than SVM. This suggests its efficiency to be used for ASD diagnosis. SHAP value gives insights into the important brain regions that contributed to the disorder and the model outcome, such as Left-Fusiform-Left-PrimMotor, which can be used as a biomarker for future investigation and treatment. The LSTM with transfer entropy underperformed due to its high computational complexity.

To improve this, other models and optimization can be used, such as Convolutional Neural Networks (CNNs) or Graph Neural Networks (GNNs), which can have less computational complexity and better generalization. In addition to that, using a bigger data size can improve the model and model generalization, or give new insights for the interpretation. These problems can also be handled using a cloud-based platform to overcome the computational demand. Finally, a clinical validation can ensure these findings.

## ● **References**

- [1] C. Lord *et al.*, "Autism spectrum disorder," *Nat. Rev. Dis. Primers*, vol. 6, p. 1, 2020. [Article Google Scholar](#)
- [2] M. Al-Beltagi, "Autism medical comorbidities," *World J. Clin. Pediatrics*, vol. 10, p. 15, 2021..[Article Google Scholar](#)
- [3] American Psychiatric Association *et al.*, *Diagnostic and Statistical Manual of Mental Disorders*, Arlington, VA, USA: American Psychiatric Association, 2013.
- [4] C. L. Alves, T. G. L. d. O. Toutain, P. de Carvalho Aguiar, *et al.*, "Diagnosis of autism spectrum disorder based on functional brain networks and machine learning," *Sci. Rep.*, vol. 13, p. 8072, 2023. doi: 10.1038/s41598-023-34650-6.<https://doi.org/10.1038/s41598-023-34650-6>
- [5] M. K. Belmonte and D. A. Yurgelun-Todd, "Functional anatomy of impaired selective attention and compensatory processing in autism," *Cogn. Brain Res.*, vol. 17, p. 651, 2003. [Article Google Scholar](#)
- [6] T. P. DeRamus, B. S. Black, M. R. Pennick, and R. K. Kana, "Enhanced parietal cortex activation during location detection in children with autism," *J. Neurodev. Disord.*, vol. 6, p. 1, 2014. [Article Google Scholar](#)
- [7] D. R. Euston, A. J. Gruber, and B. L. McNaughton, "The role of medial prefrontal cortex in memory and decision making," *Neuron*, vol. 76, p. 1057, 2012. [Article CAS PubMed PubMed Central Google Scholar](#)
- [8] D. P. Kennedy, E. Redcay, and E. Courchesne, "Failing to deactivate: Resting functional abnormalities in autism," *Proc. Natl. Acad. Sci. U.S.A.*, vol. 103, p. 8275, 2006. [Article ADS CAS PubMed PubMed Central Google Scholar](#)
- [9] T. A. Keller, R. K. Kana, and M. A. Just, "A developmental study of the structural integrity of white matter in autism," *NeuroReport*, vol. 18, p. 23, 2007. [Article PubMed Google Scholar](#)
- [10] Y. Aoki, O. Abe, Y. Nippashi, and H. Yamasue, "Comparison of white matter integrity between autism spectrum disorder subjects and typically developing individuals: A meta-analysis," *Mol. Autism*, vol. 4, p. 1, 2013. [Article Google Scholar](#)
- [11] F. De Vico Fallani *et al.*, "Multiple pathways analysis of brain functional networks from EEG signals: An application to real data," *Brain Topogr.*, vol. 23, p. 344, 2011. [Article PubMed Google Scholar](#)
- [12] C. L. Alves, A. M. Pineda, K. Roster, C. Thielemann, and F. A. Rodrigues, "EEG functional connectivity and deep learning for automatic diagnosis of brain disorders: Alzheimer's disease and schizophrenia," *J. Phys. Complex.*, vol. 3, p. 025001, 2022. [Article ADS Google Scholar](#)

- [13] V. Menon and S. Crottaz-Herbette, "Combined EEG and FMRI studies of human brain function," *Int. Rev. Neurobiol.*, vol. 66, p. 291, 2005. [Article](#) [CAS](#) [PubMed](#) [Google Scholar](#)
- [14] M. J. Sturzbecher, "Detecção e caracterização da resposta hemodinâmica pelo desenvolvimento de novos métodos de processamento de imagens funcionais por ressonância magnética," Ph.D. dissertation, Univ. São Paulo, São Paulo, Brazil, 2006.
- [15] B. Biswal, F. Z. Yetkin, V. M. Haughton, and J. S. Hyde, "Functional connectivity in the motor cortex of resting human brain using echo-planar MRI," *Magn. Reson. Med.*, vol. 34, p. 537, 1995. [Article](#) [CAS](#) [PubMed](#) [Google Scholar](#)
- [16] I. Ekanayake, D. Meddage, and U. Rathnayake, "A novel approach to explain the black-box nature of machine learning in compressive strength predictions of concrete using Shapley additive explanations (SHAP)," *Case Stud. Constr. Mater.*, vol. 17, p. e01059, 2022.
- [17] A. R. Ferguson, J. L. Nielson, M. H. Cragin, A. E. Bandrowski, and M. E. Martone, "Big data from small data: Data-sharing in the 'long tail' of neuroscience," *Nat. Neurosci.*, vol. 17, p. 1442, 2014. [Article](#) [CAS](#) [PubMed](#) [PubMed Central](#) [Google Scholar](#)
- [18] H.-J. Bae *et al.*, "A Perlin noise-based augmentation strategy for deep learning with small data samples of HRCT images," *Sci. Rep.*, vol. 8, p. 1, 2018. [Article](#) [ADS](#) [Google Scholar](#)
- [19] American Psychiatric Association, *Diagnostic and Statistical Manual of Mental Disorders*, 5th ed. Arlington, VA, USA: American Psychiatric Publishing, 2013.
- [20] C. Lord, M. Elsabbagh, G. Baird, and J. Veenstra-Vanderweele, "Autism spectrum disorder," *Lancet*, vol. 392, no. 10146, pp. 508–520, Aug. 2018.
- [21] M. A. Just, V. L. Cherkassky, T. A. Keller, and N. J. Minshew, "Cortical activation and synchronization during sentence comprehension in high-functioning autism: Evidence of underconnectivity," *Brain*, vol. 127, no. 8, pp. 1811–1821, Aug. 2004.
- [22] F. Pereira, T. Mitchell, and M. Botvinick, "Machine learning classifiers and fMRI: A tutorial overview," *NeuroImage*, vol. 45, no. 1, Suppl. 1, pp. S199–S209, Mar. 2009.
- [23] B. B. Biswal, F. Z. Yetkin, V. M. Haughton, and J. S. Hyde, "Functional connectivity in the motor cortex of resting human brain using echo-planar MRI," *Magn. Reson. Med.*, vol. 34, no. 4, pp. 537–541, Oct. 1995.
- [24] A. Di Martino *et al.*, "The autism brain imaging data exchange: Towards a large-scale evaluation of the intrinsic brain architecture in autism," *Mol. Psychiatry*, vol. 19, no. 6, pp. 659–667, Jun. 2014.

- [25] N. Tzourio-Mazoyer *et al.*, "Automated anatomical labeling of activations in SPM using a macroscopic anatomical parcellation of the MNI MRI single-subject brain," *NeuroImage*, vol. 15, no. 1, pp. 273–289, Jan. 2002.
- [26] E. T. Rolls, C.-C. Huang, C.-P. Lin, J. Feng, and M. Joliot, "Automated anatomical labelling atlas 3," *NeuroImage*, vol. 202, p. 116189, 2019.
- [27] P. Bellec, P. Rosa-Neto, O. C. Lyttelton, H. Benali, and A. C. Evans, "Multi-level bootstrap analysis of stable clusters in resting-state fMRI," *NeuroImage*, vol. 51, no. 3, pp. 1126–1139, Jul. 2010.
- [28] X. Yang, N. Zhang, and P. Schrader, "A study of brain networks for autism spectrum disorder classification using resting-state functional connectivity," *Mach. Learn. Appl. (MLWAI)*, vol. 3, p. 100290, 2022.
- [29] C. Spearman, "The proof and measurement of association between two things," *Am. J. Psychol.*, vol. 15, no. 1, pp. 72–101, Jan. 1904.
- [30] L. Liu, B. Li, and D. Hu, "Autism spectrum disorder studies using fMRI data and machine learning: A review," *Front. Neurosci.*, vol. 15, p. 697870, 2021.
- [31] C. L. Alves *et al.*, "Multiclass classification of Autism Spectrum Disorder, attention deficit hyperactivity disorder, and typically developed individuals using fMRI functional connectivity analysis," *PLOS One*, vol. 19, no. 10, p. e0305630, Oct. 2024.
- [32] T. Schreiber, "Measuring information transfer," *Phys. Rev. Lett.*, vol. 85, no. 2, pp. 461–464, Jul. 2000.
- [33] M. Wibral, B. Rahm, M. Rieder, M. Lindner, R. Vicente, and J. T. Lizier, "Transfer entropy in magnetoencephalographic data: Quantifying information flow in cortical command and execution networks," *Prog. Biophys. Mol. Biol.*, vol. 105, no. 1–2, pp. 80–97, Apr. 2011.
- [34] R. M. Hutchison *et al.*, "Dynamic functional connectivity: Promise, issues, and interpretations," *NeuroImage*, vol. 80, pp. 360–378, Oct. 2013.
- [35] S. Hochreiter and J. Schmidhuber, "Long short-term memory," *Neural Comput.*, vol. 9, no. 8, pp. 1735–1780, Nov. 1997.

